Quantum illumination with photon-subtracted continuous-variable entanglement

ShengLi Zhang,[1,2] JianSheng Guo,[1] WanSu Bao,[1] JianHong Shi,[1] ChenHui Jin,[1] XuBo Zou,[2] and GuangCan Guo[2]
[1]*Zhengzhou Information Science and Technology Institute, Zhengzhou 450004, China*
[2]*Key Laboratory of Quantum Information, University of Science and Technology of China (CAS), Hefei 230026, China*
(Received 30 March 2014; published 9 June 2014)

Quantum illumination is a protocol where quantum resources are utilized to detect a low-reflectivity object embedded in a bright thermal noise bath. For example, quantum illumination with a two-mode squeezed state (TMSS) provides a 6 dB advantage in the error-probability exponent over the optimal classical illumination. We here consider quantum illumination with the photon-subtracted two-mode squeezed state (PSTMSS). Our result is twofold. First, we show that a much smaller error probability $P_{\rm err}$ could be obtained, meaning that much smaller resources will be required in quantum illumination for a fixed $P_{\rm err}$. Second, quantum illumination with PSTMSS appreciably outperforms its classic correspondence in both low- and high-noise operating regimes, extending the regimes in which quantum illumination is optimal for target detection.

DOI: 10.1103/PhysRevA.89.062309 PACS number(s): 03.67.Bg, 42.50.Ex, 03.67.Hk, 03.67.Mn

I. INTRODUCTION

Quantum precise measurement [1], quantum teleportation [2], and quantum computation [3] are important quantum technologies which challenge current wisdom about the limit and power of conventional informational processing. However, environment-induced decoherence quickly destroys the quantum entanglement underlying these techniques and thus substantially undermines any enhancement in the quantum technique. Remarkably, quantum illumination, or more precisely quantum target detection, with its foundation based on bipartite nonclassical correlation is quite an exception. Lloyd shows that even in entanglement-destroying loss and noise, one can still make substantial improvement in the signal-to-background ratio in realistic target detections [4].

The paradigm of Lloyd's quantum illumination is as follows. To detect a region where a low-reflectivity object may be embedded, we prepare two entangled optical modes. One is sent to irradiate the region and the other is retained as the ancilla. Then when the light is received from the region, we perform the optimal joint measurement on the received light and the ancilla, achieving an effective signal-to-background ratio of $2\eta/b$, with $\eta \ll 1$ being the reflectivity of the object and b being the average number of photons in thermal noise. As a comparison, the signal-to-background ratio in illumination with an unentangled single photon follows η/b. Such an original idea has been further investigated in several theories and experiments. Shapiro and Lloyd explored the performance gain of quantum illumination in the multiphoton regime [5]. Tan *et al.* provide a full Gaussian-state treatment of quantum-illumination target detection [6]. Guha *et al.* present two structured optical receivers that can be readily implemented in proof-of-concept experiments [7]. More recently, a quantum-illumination experiment, although slightly different from Lloyd's original one, has been carried out and it showed that illumination with quantum protocol has clear advantages over classical ones, i.e., based on classical correlations [8].

The aim of this paper is to investigate the application of a photon-subtraction technique for object detection. We consider the photon-subtracted two-mode squeezed state (PSTMSS) as the basic quantum resource and evaluate the corresponding minimal error probability in target detection. Actually, the photon-subtracted state is a non-Gaussian state and our study can be considered as the natural extension of quantum illumination from Gaussian to non-Gaussian regimes. Numerical result shows that like their advantage in quantum-state distillation [9–11] and quantum-error correction [12], non-Gaussian quantum states support much lower error probability and are more robust against environmental noise.

This paper is organized as follows. In Sec. II, we introduce the model of quantum illumination with a photonic beam splitter. In Sec. III, we consider the ideal photon-subtracted TMSS state and derive the relevant error probability. Indeed, ideal photon-subtracted TMSS is obtained theoretically by applying bi-side photon annihilation operators on the entangled two-mode state. In laboratories, the practical PSTMSS state obtained by beam-splitter coupling and on-off photon detectors is more often discussed. Likewise, in Sec. IV we just consider the practical PSTMSS state. Finally, the conclusions are drawn in Sec. V.

II. QUANTUM-ILLUMINATION MODEL

Here, let us present the model of quantum illumination with a beam splitter. Typical quantum illumination can be explicitly shown as in Fig. 1(a). One mode of the entangled photonic modes, say B, is used to interrogate the unknown object hidden in the background. The reflectivity of the object, denoted with κ, is far less than 1 due to photon loss during both up and down transmission and low-efficiency in photon detectors. Finally, after receiving photons from the region, we will perform joint quantum measurement on the retrieved light and the ancilla. Conceivably, the optimal quantum joint measurement could help to provide sufficient information to make a judgment on the presence of the unknown target. In fact, when the target exists, one may have a rather small reflectivity $\kappa \ll 1$. However, when the target is absent, we have $\kappa = 0$. Thus, the task of joint quantum measurement is to make a state discrimination between the two-mode quantum state: $\rho_{\rm AB}^{(1)}$ (target exists) and $\rho_{\rm AB}^{(0)}$(target does not exist). The optimal discrimination takes place in the process of joint quantum measurement, which returns a dichotic result:

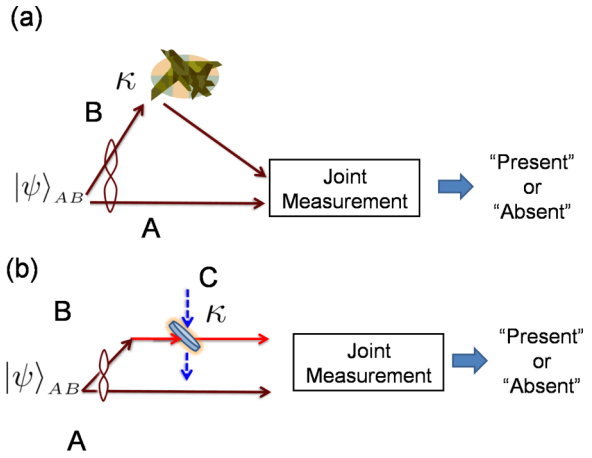

FIG. 1. (Color online) (a) Schematic diagram of quantum target detection of low-reflectivity object. (b) Simulation of quantum illumination with a photonic beam splitter, with transmittance κ and thermal state in C mode. Joint quantum measurement is of paramount importance in performance enhancement. The result of quantum measurement provides dichotic information required for target detection.

1 or 0, corresponding to the existence or absence of the target.

The joint quantum measurement can be mathematically formulated with the positive operator valued measurement (POVM), usually characterized with a set of positive operators $\{E_r\}$ $(r = 0,1)$. Quantum measurement is a kind of probabilistic measurement and for arbitrary quantum state ρ, the detecting result is in essence probabilistic, with the probability given by

$$P_1 = \mathrm{Tr}[\rho E_1], \quad P_0 = \mathrm{Tr}[\rho E_0]. \tag{1}$$

The normalization of the probability $P_0 + P_1 = 1$ follows directly from the trace-preserving condition in POVM: $E_0 + E_1 = I$, with I being the identity matrix in the Hilbert space $H_{\dim(\rho)}$.

We consider the most general scenario in which we have no information on the target. We assume the two hypotheses that the region may or may not contain a target are equally likely, i.e., the *a priori* probability

$$p_0 = \mathrm{Prob}(\text{target absent}) = \tfrac{1}{2}, \tag{2}$$

$$p_1 = \mathrm{Prob}(\text{target exist}) = 1 - p_0 = \tfrac{1}{2}. \tag{3}$$

Averaging over both hypotheses, one may find that the error probability is

$$\begin{aligned} P_{\mathrm{err}} &= p_1 \mathrm{Tr}\big[\rho_{\mathrm{AB}}^{(1)} E_0\big] + p_0 \mathrm{Tr}\big[\rho_{\mathrm{AB}}^{(0)} E_1\big] \\ &= \tfrac{1}{2}\big(1 - \tfrac{1}{2}\mathrm{Tr}\big[(\rho_{\mathrm{AB}}^{(1)} - \rho_{\mathrm{AB}}^{(0)})(E_1 - E_0)\big]\big). \end{aligned} \tag{4}$$

The construction of optimal $\{E_r\}$ for discriminating a nonorthogonal quantum state has been clearly understood [13–15] and the minimal error probability is

$$P_{\mathrm{err}} = \tfrac{1}{2}\big(1 - \tfrac{1}{2}\big\|\rho_{\mathrm{AB}}^{(1)} - \rho_{\mathrm{AB}}^{(0)}\big\|\big), \tag{5}$$

with $\|\gamma\| = \mathrm{Tr}\sqrt{\gamma^\dagger \gamma} = \sum_i s_i(\gamma)$, and $s_i(\gamma)$ is the absolute value of the eigenvalues [14].

To see the advantage of quantum illumination with PSTMSS and TMSS, one should evaluate P_{err} when $|\psi\rangle_{\mathrm{PSTMSS}}$ and $|\psi\rangle_{\mathrm{TMSS}}$ as input. Correspondingly, we may obtain the error probability $P_{\mathrm{err}}^{\mathrm{PSTMSS}}$ and $P_{\mathrm{err}}^{\mathrm{TMSS}}$. However, only a moment's thought is needed to find that $P_{\mathrm{err}}^{\mathrm{PSTMSS}}$ and $P_{\mathrm{err}}^{\mathrm{TMSS}}$ are both close to $1/2$ for our quantum-illumination scheme in Fig. 1.

To see the effect gained by quantum more clearly, a joint state of many-copy entanglement will always be applied [4–6]. Then, the error probability with an M copy state is

$$P_{\mathrm{err},M} = \tfrac{1}{2}\big(1 - \tfrac{1}{2}\big\|\rho_{\mathrm{AB}}^{(1)\otimes M} - \rho_{\mathrm{AB}}^{(0)\otimes M}\big\|\big). \tag{6}$$

At this point, the optimal joint measurement POVM giving the judgment rule should be the projectors on the support of the positive and negative parts of $\rho_{\mathrm{AB}}^{(1)\otimes M} - \rho_{\mathrm{AB}}^{(0)\otimes M}$.

Direct evaluation of $P_{\mathrm{err},M}$ is quite a difficult task when the dimensions of ρ_{AB} and M are very large. Fortunately, the quantum Chernoff bound (QCB) [16,17] comes to the rescue. For discrimination of the two states $\rho_{\mathrm{AB}}^{(1)\otimes M}$ and $\rho_{\mathrm{AB}}^{(0)\otimes M}$, the QCB places the following limit on the error probability:

$$P_{\mathrm{err},M} \leqslant P_{\mathrm{QCB}}^{M} = \tfrac{1}{2} e^{-M\mathcal{E}} = \tfrac{1}{2}\Big\{\min_{0\leqslant s\leqslant 1} Q_s\Big\}^{M}, \tag{7}$$

with

$$\mathcal{E} = -\ln\Big[\min_{0\leqslant s\leqslant 1} Q_s\Big], \quad Q_s = \mathrm{Tr}\big[\rho_{\mathrm{AB}}^{(1)s}\rho_{\mathrm{AB}}^{(0)1-s}\big]. \tag{8}$$

P_{QCB}^{M} poses an upper bound on the error probability of quantum target detection with joint quantum measurement on arbitrary M copies. More important, such a QCB can be conveniently obtained with the calculation involving single-copy states $\rho_{\mathrm{AB}}^{(1)}$ and $\rho_{\mathrm{AB}}^{(0)}$. On the other hand, the lower bound of $P_{\mathrm{err},M}$ is also an important figure of merit. A computable lower bound is given by [6]

$$P_{\mathrm{err},M} \geqslant P_{\mathrm{err},M,L} = \tfrac{1}{2}\Big(1 - \sqrt{1 - \big\{\mathrm{Tr}\big[\rho_{\mathrm{AB}}^{(1)1/2}\rho_{\mathrm{AB}}^{(0)1/2}\big]\big\}^{2M}}\Big). \tag{9}$$

The importance of $P_{\mathrm{err},M,L}$ lies in the fact that it is again a given quantity evaluated from single-copy states $\rho_{\mathrm{AB}}^{(1)}$ and $\rho_{\mathrm{AB}}^{(0)}$. Although not exponentially tight, $P_{\mathrm{err},M,L}$ and P_{QCB}^{M} do provide clues to how P_{err}^{M} behaves with exponentially growing M. In the following, we will consider the specific scenarios in which the ideal PSTMSS and practical PSTMSS are involved.

III. QUANTUM ILLUMINATION WITH IDEAL PSTMSS

We now consider the quantum illumination with the state of ideal PSTMSS. First of all, we consider the quantum state of TMSS. In Ref. [6], TMSS is described with a covariance matrix in phase space. Here, instead, our analysis will start from the photon number space. In fact, the formalism in Ref. [6] applies solely to a Gaussian state. In the non-Gaussian regime, for example, the photon-subtracted TMSS, the photon state space

is most powerful and straightforward. To this point, we use the Fock state [18] $\{|n\rangle, n = 0,1,\ldots,\infty\}$ as a basis for the quantum state of the single-mode Hilbert space. For example, the TMSS state is a superposition of infinitely many Fock states in photon number space

$$|\Psi\rangle_{\rm AB} = \sqrt{1-\lambda^2}\sum_{n=0}^{\infty}\lambda^n|n\rangle_{\rm A}|n\rangle_{\rm B}. \tag{10}$$

Photon-subtracted TMSS is a modified TMSS and is what we are mainly concerned with in the following discussions. Photon subtraction is not completely new but frequently used in continuous-variable entanglement distillation [19–27] and Bell-inequality violation [28–30]. Mathematically, ideal photon subtraction can be represented with the photon annihilation operator $\hat{a}$ and PSTMSS follows $\hat{a}_{\rm A}\otimes\hat{a}_{\rm B}|\Psi\rangle_{\rm AB}$. After normalization, we obtain

$$|\Psi'\rangle_{\rm AB} = \sum_{n=0}^{\infty}\frac{(1-\lambda^2)^{3/2}}{\sqrt{1+\lambda^2}}(n+1)\lambda^n|n,n\rangle, \tag{11}$$

with $\lambda = \tanh(r)$ and r being the squeezing parameters.

We now consider the derivation of $\rho_{\rm AB}^{(1)}$ and $\rho_{\rm AB}^{(0)}$. First, when the target is absent we have $\kappa = 0$ and the reflectivity of the beam splitter [Fig. 1(b)] is unity. All the thermal states in mode C will be projected onto the joint quantum measurement. Thus, we have

$$\begin{aligned}\rho_{\rm AB}^{(0)} &= {\rm Tr}_{\rm B}[|\Psi'\rangle_{\rm AB}\langle\Psi'|]\otimes\rho_{\rm th}(N_{\rm B})\\ &= \frac{(1-\lambda^2)^3}{(1+\lambda^2)}\sum_{n=0}^{\infty}\lambda^{2n}(n+1)^2|n\rangle\langle n|\otimes\rho_{\rm th}(N_{\rm B}),\end{aligned} \tag{12}$$

with $\rho_{\rm th}(N_{\rm B})$ being the single-mode thermal state with average photon number $N_{\rm B}$:

$$\rho_{\rm th}(N_{\rm B}) = \sum_{k=0}^{\infty}\frac{1}{N_{\rm B}+1}\left(\frac{N_{\rm B}}{N_{\rm B}+1}\right)^k|k\rangle\langle k|. \tag{13}$$

Second, when the target is present, we have a beam splitter of extremely low transmittance κ. The unitary transformation of modes B and C is described with $\widetilde{V} = \exp\{\arctan[\sqrt{(1-\eta)/\eta}](\hat{a}_{\rm B}\hat{a}_{\rm C}^\dagger - \hat{a}_{\rm B}^\dagger\hat{a}_{\rm C})\}$. Written in the Fock basis $|n\rangle_{\rm A}|m\rangle_{\rm B}$, the transformation of $\widetilde{V}$ follows

$$\widetilde{V}|n\rangle|m\rangle = \sum_{k=0}^{n}\sum_{\ell=0}^{m}f_{kl}^{nm}(\eta)|n-k+\ell\rangle|m+k-\ell\rangle, \tag{14}$$

with

$$\begin{aligned}f_{kl}^{nm}(\eta) = (-1)^\ell&\sqrt{\binom{n}{k}\binom{n-k+\ell}{\ell}\binom{m}{\ell}\binom{m+k-\ell}{k}}\\ &\times(\eta)^{\frac{m+n-k-\ell}{2}}(1-\eta)^{\frac{k+\ell}{2}}.\end{aligned} \tag{15}$$

Thus, the coupling between the three-mode state ABC follows

$$\rho_{\rm ABC} = \widetilde{V}[|\Psi'\rangle\langle\Psi'|\otimes\rho_{\rm th}(N_{\rm B}')]\widetilde{V}^\dagger,$$

in which we use a thermal state with slightly different intensity $N_{\rm B}' = \frac{N_{\rm B}}{1-\kappa}$ to represent the noise entering mode C. Such a choice is made in order to specify the thermal noise observed in joint quantum measurement the same as the one when target is absent [6].

Finally at the joint measurement, we only take care of modes A and B. By taking a partial trace over mode C, we have

$$\begin{aligned}\rho_{\rm AB}^{(1)} = {\rm Tr}_{\rm C}[\rho_{\rm ABC}] = \frac{(1-\lambda^2)^3}{\lambda^2(1+\lambda^2)(N_{\rm B}'+1)}&\sum_{n_1=0}^{\infty}\sum_{n_2=0}^{\infty}\sum_{m=0}^{\infty}\frac{1}{N_{\rm B}'+1}\left(\frac{N_{\rm B}'}{N_{\rm B}'+1}\right)^k\lambda^{n_1+n_2+2}(n_1+1)(n_2+1)|n_1\rangle_{\rm A}\langle n_2|\\ \otimes\left(\sum_{k=0}^{n_1}\sum_{\ell=0}^{m}\sum_{k'=0}^{n_2}\sum_{\ell'=0}^{m}f_{k,\ell}^{n_1 m}(\kappa)f_{k'\ell'}^{n_2 m}(\kappa)\delta_{k-\ell,k'-\ell'}|n_1-k+\ell\rangle_{\rm B}\langle n_2-k'+\ell'|\right).\end{aligned} \tag{16}$$

From Eqs. (12) and (16), we can immediately evaluate the corresponding Q_s via numerical methods. Precisely, we cannot save and process all the entries in the density matrix of infinite-dimensional Hilbert space and one convenient way is to truncate the photon number of the relevant quantum state to a preassigned value $\overline{D}$. Namely, we consider the photon number subspace $0,1,\ldots,\overline{D}-1$ and neglect all the contributions of higher photon number. Such an approximation is quite suitable particularly when the input entanglement $|\Psi'_{\rm AB}\rangle$ is rather weak. Of course, the larger the value $\overline{D}$, the more information of $\rho_{\rm AB}^{(0)}$ and $\rho_{\rm AB}^{(1)}$ will be preserved. In fact, to balance with the computer resources required in the numerical simulation and numerical convergence, a suitable $\overline{D}$ is chosen for numerical computation.

The advantage afforded by photon subtraction can be clearly observed by showing the dependence of the QCB for $P_{{\rm err},M}$ on the number of copies M. The plots are given in logarithmic scales in Fig. 2. For clarity, we show the QCB in three different values of environment noise: (a) $N_{\rm B} = 10$, (b) $N_{\rm B} = 1$, and (c) $N_{\rm B} = 0.1$. Also shown is the lower bound for error probability of detection with coherent state $|\alpha\rangle$ (classic illumination) and TMSS (quantum illumination) [6]. In each curve (a)–(c), we choose target reflectivity to be $\kappa = 0.01$, the average of photon number in transmitted mode $N_s = 0.01$. Moreover, the parameter for the TMSS to be photon subtracted still follows $N_s = 0.01$. This helps us to clearly show the enhancement afforded by photon subtraction. The solid lines in Fig. 2 denote the QCB of target detection with PSTMSS. Our numerical results are summarized as follows:

(1) The QCB for PSTMSS is not only much smaller than that for TMSS, $P_{\rm QCB}^{M,{\rm PSTMSS}} < P_{\rm QCB}^{M,{\rm TMSS}}$, but also far less than the lower bound of TMSS, $P_{\rm QCB}^{M,{\rm PSTMSS}} < P_{{\rm err},M,L}^{M,{\rm TMSS}}$. This tells us that even if the QCB fails to be exponentially tight, the error probability $P_{\rm QCB}^{M,{\rm PSTMSS}}$ is strictly smaller than

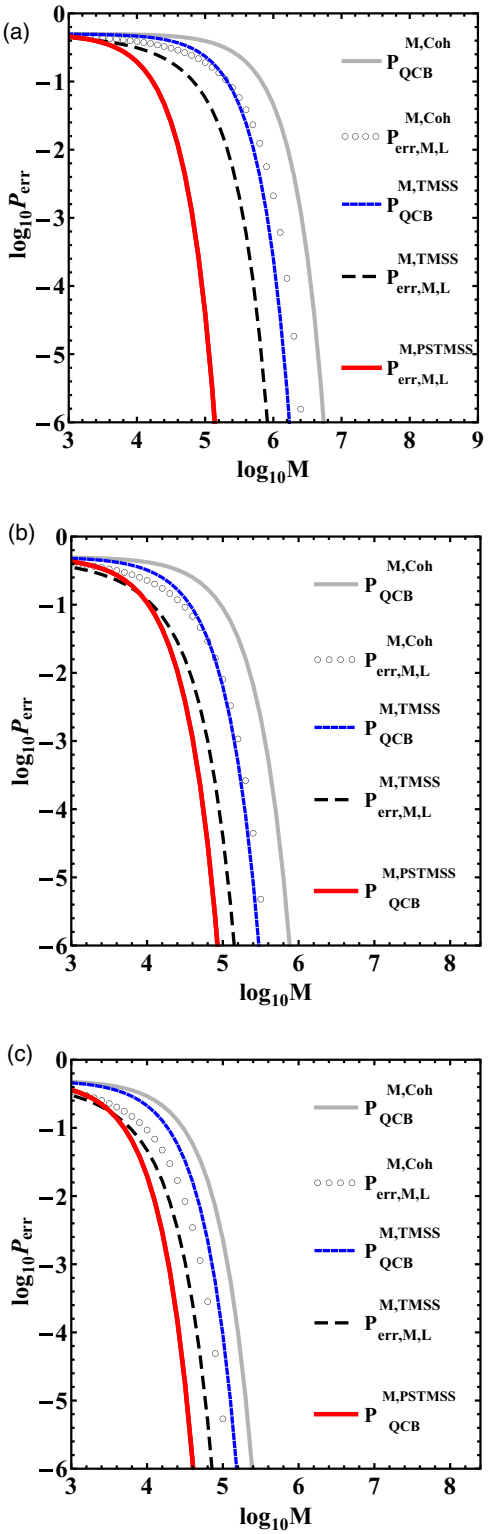

FIG. 2. (Color online) Error probability of target detection for coherent state, TMSS state, and PSTMSS. (a) $N_B = 10$, $\overline{D} = 20$, (b) $N_B = 1$, $\overline{D} = 15$, (c) $N_B = 0.1$, $\overline{D} = 10$. Also shown are the lower bounds for the coherent (circle lines) and TMSS (dashed lines) states. The reflectivity of the target (equivalently, the transmittance coefficient of the beam splitter) is chosen: $\kappa = 0.01$. For all subplots in (a)–(c), the transmitted modes of the TMSS and coherent states are chosen to be $N_s = 0.01 = \sinh^2(r) = |\alpha|^2$. Also in PSTMSS, the squeezing parameter for the relevant TMSS still follows $N_s = 0.01$.

$P^{M,TMSS}_{err,M,L}$, showing the power of quantum illumination with photon-subtracted Gaussian state.

(2) Gaussian quantum illumination with TMSS outperforms the classic receiver (the classic illumination) in strong noisy backgrounds [see Fig. 2(a)]. However, in less noisy circumstances, for example, $N_B = 1$ or $N_B = 0.1$, the quantum illumination with TMSS is no longer the optimal receiver, which is explicitly demonstrated in Figs. 2(b) and 2(c). One could see that the QCB of $P^{M,TMSS}_{QCB}$ even exceeds the lower bound of the coherent state, and the advantage of quantum illumination disappears. Fortunately, the photon-subtracted state helps even in less noisy environments.

This leads us to investigate the mechanism under which error probability has been reduced. As shown in Eq. (8), the error probability in the case of a many-copy state is not determined by the entanglement in the quantum state of ρ_{AB} but by the distinction between the two states $\rho^{(1)}_{AB}$ and $\rho^{(0)}_{AB}$. In terms of the quantum Chernoff bound, such a distinction is further evaluated with the corresponding overlap $Q^{TMSS}_s = \mathrm{Tr}[\rho^{(1)\,s}_{AB}\,\rho^{(0)\,1-s}_{AB}]$. Whereas in the case of coherent-state illumination, we have no B mode and $Q^{coh}_s = \mathrm{Tr}[\rho^{(1)s}_{A}\,\rho^{(0)\,1-s}_{A}]$. In a less noisy environment such as $N_B = 0.1$, it can be numerically shown that $\min_{0\leqslant s\leqslant 1} Q^{TMSS}_s = Q^{TMSS}_{0.5}$ and $\min_{0\leqslant s\leqslant 1} Q^{Coh}_s = Q^{Coh}_{0.5}$ and $Q^{TMSS}_{0.5} > Q^{Coh}_s$ and coherent-state illumination (classic illumination with no entanglement) performs better than quantum-state illumination (with TMSS entanglement state), which is independently observed in Ref. [5].

As for the state PSTMSS, it appears that error probability with PSTMSS is always lower than with TMSS. The reason can be tracked back to the photon-number population in Eq. (11). Actually, we use a very weak TMSS state ($N_s = 0.01$), which can be well approximated with $|\psi_{TMSS}\rangle = |00\rangle + \sqrt{N_s}|11\rangle$. However, with bi-side photon subtraction, we obtain the state $|\psi^{PS}_{TMSS}\rangle = |00\rangle + 2\sqrt{N_s}|11\rangle$. This equals a pure TMSS state with doubled average photon number. Namely, this seems as if we use a squeezing-double TMSS state to illuminate the target. The error probability is no doubt reduced. It should be noted that the doubled squeezing comes from our photon subtraction which modulates the photon-number distribution, not from simply increasing the average photon number N_s. This again shows the effect of photon subtraction in quantum target detection. It appreciably extends the regimes in which quantum illumination is optimal for target detection.

IV. QUANTUM ILLUMINATION WITH PRACTICAL PSTMSS

In the previous section, we considered quantum illumination with ideal photon subtraction. Physically, these are nonphysical operations and the realistic photon annihilation can be implemented with photonic beam splitters and "on-off" photon detectors [19,21]. Actually, this is the one of the most widely used techniques in continuous-variable entanglement distillation. After the realistic photon subtraction, a pure TMSS state is projected into a mixed state. The mix is introduced by the nondiscrimination of the detected photons. According to Refs. [19,23], the state after photon subtraction can be

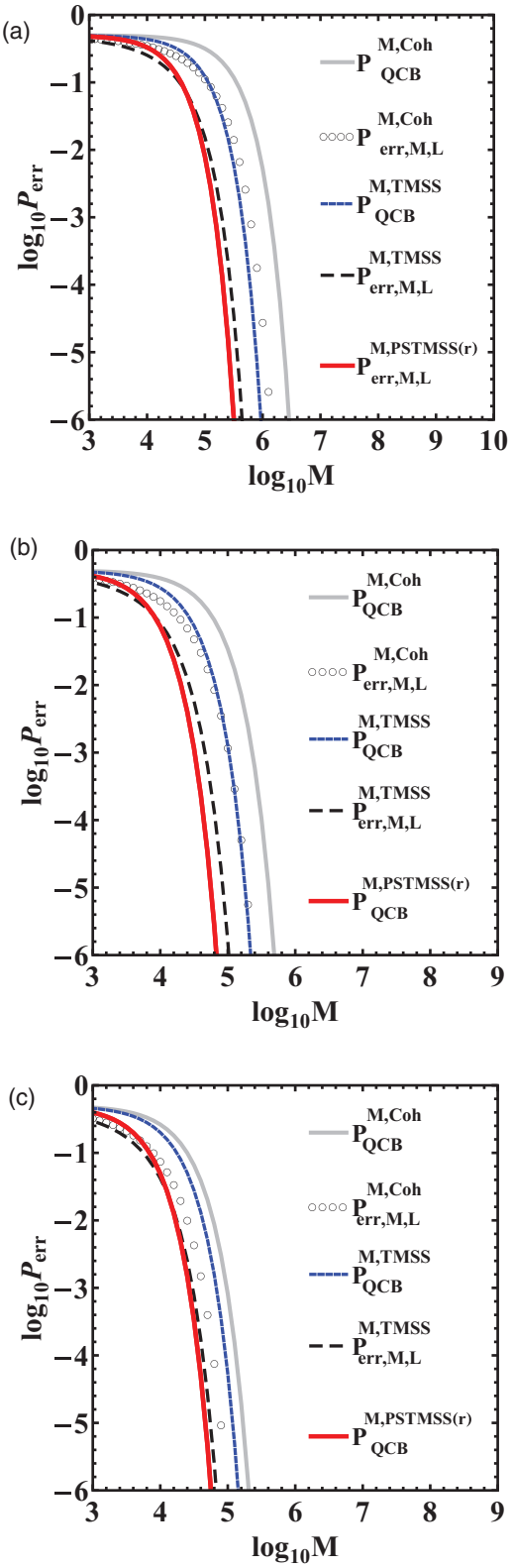

FIG. 3. (Color online) Error probability of target detection for coherent state, TMSS state, and realistic PSTMSS state. (a) $N_B = 5$, $\overline{D} = 25$ (b) $N_B = 0.5$, $\overline{D} = 17$, (c) $N_B = 0.05$, $\overline{D} = 10$. Also shown are the lower bounds for coherent (circle lines) and TMSS (dashed lines) states. All other parameters are chosen from Fig. 2.

represented with

$$\rho_{AB}^{\mathrm{PSTMSS}(r)} = \frac{(1-\lambda^2)(1-\lambda^2 T)(1-\lambda^2 T^2)}{\lambda^2(1-T)^2(1+\lambda^2 T)} \sum_{n,m=1}^{\infty} (\lambda T)^{n+m} \times \sum_{k,l=1}^{\min(n,m)} C_{mn}^{kl} |n-k, n-l\rangle\langle m-k, m-l|, \tag{17}$$

with

$$C_{mn}^{kl} = \sqrt{\binom{n}{k}\binom{m}{k}\binom{n}{l}\binom{m}{l}} \left(\frac{1-T}{T}\right)^{k+l}, \tag{18}$$

and T being the transmittance of the beam splitter in photon subtractions. The "(r)" in Eq. (17) indicates that the state is now a realistic PSTMSS state. Then the quantum illumination with $\rho_{AB}^{\mathrm{PSTMSS}(r)}$ can proceed the same way as the one in Sec. III. When the target is absent, it follows

$$\rho_{\mathrm{AB}(r)}^{(0)} = \mathrm{Tr}_B\left[\rho_{AB}^{\mathrm{PSTMSS}(r)}\right] \otimes \rho_{\mathrm{th}}(N_B). \tag{19}$$

However, when the target is present, we have

$$\rho_{\mathrm{AB}(r)}^{(1)} = \mathrm{Tr}_C\left\{\widetilde{V}\left[\rho_{AB}^{\mathrm{PSTMSS}(r)} \otimes \rho_{\mathrm{th}}(N_B')\right]\widetilde{V}^{\dagger}\right\}. \tag{20}$$

With Eqs. (19) and (20), we can numerically calculate $Q_s = \mathrm{Tr}[\rho_{AB(r)}^{(1)s}\rho_{AB(r)}^{(0)1-s}]$ and then evaluate the QCB in quantum illumination. In Fig. 3, we compare the performance of quantum illumination with realistic photon subtraction. Here, the transmittance of the beam splitter is chosen as $T = 0.95$, which has already been checked in a recent experiment [27]. We give a numerical evaluation of the performance of quantum illumination with a practical photon-subtracted state. Here, to keep the numerical convergence for simulating the mixed state [Eq. (17)], we keep more photons in each mode. Again, our result shows that the illumination with a realistic photon-subtracted state still works very well to improve quantum illumination, in both low- and high-noise operating regimes.

V. CONCLUSIONS

We demonstrate that a photon-subtracted (both ideal and realistic) continuous-variable entanglement state can be applied to the detection of a low-reflectivity object in noisy and noiseless environments. Our result is obtained via the derivation of a non-Gaussian quantum state in photon-number space. This is a complement to the previous result for quantum illumination with Gaussian states, and these non-Gaussian states can be generated in laboratories [31]. We hope our extension of the regime where quantum illumination outperforms the classic illumination can be experimentally checked in the near future.

ACKNOWLEDGMENTS

The authors acknowledge National Natural Science Foundation of China (Grants No. 11204197, No. 11204379, and No. 11074244), also by financial support from the National 973 Fundamental Research Program (Grant No. 2011cba00200) and the Doctor Foundation of Education Ministry of China (Grant No. 20113402110059).

[1] V. Giovannetti, L. Maccone, and S. Lloyd, Science **306**, 1330 (2004).
[2] C. H. Bennett, G. Brassard, C. Crépeau, R. Jozsa, A. Peres, and W. K. Wootters, Phys. Rev. Lett. **70**, 1895 (1993).
[3] P. W. Shor, in *Proceedings of the 35th Annual Symposium on the Foundations of Computer Science*, edited by S. Goldwasser (IEEE Computer Society Press, Los Alamitos, CA, 1994), p. 124.
[4] S. Lloyd, Science **321**, 1463 (2008).
[5] J. H. Shapiro and S. Lloyd, New J. Phys. **11**, 063045 (2009).
[6] Si-Hui Tan, Baris I. Erkmen, Vittorio Giovannetti, Saikat Guha, Seth Lloyd, Lorenzo Maccone, Stefano Pirandola, and Jeffrey H. Shapiro, Phys. Rev. Lett. **101**, 253601 (2008).
[7] Saikat Guha and Baris I. Erkmen, Phys. Rev. A **80**, 052310 (2009).
[8] E. D. Lopaeva, I. Ruo Berchera, I. P. Degiovanni, S. Olivares, G. Brida, and M. Genovese, Phys. Rev. Lett. **110**, 153603 (2013).
[9] J. Eisert, S. Scheel, and M. B. Plenio, Phys. Rev. Lett. **89**, 137903 (2002).
[10] J. Fiurášek, Phys. Rev. Lett. **89**, 137904 (2002).
[11] G. Giedke and J. I. Cirac, Phys. Rev. A **66**, 032316 (2002).
[12] Julien Niset, Jaromír Fiurášek, and Nicolas J. Cerf, Phys. Rev. Lett. **102**, 120501 (2009).
[13] C. W. Helstrom, Int. Control **10**, 254 (1967).
[14] M. F. Sacchi, Phys. Rev. A **71**, 062340 (2005).
[15] M. F. Sacchi, Phys. Rev. A **72**, 014305 (2005).
[16] K. M. R. Audenaert, J. Calsamiglia, R. Mũnoz-Tapia, E. Bagan, L. Masanes, A. Acin, and F. Verstraete, Phys. Rev. Lett. **98**, 160501 (2007).
[17] J. Calsamiglia, R. Mũnoz-Tapia, L. Masanes, A. Acin, and E. Bagan, Phys. Rev. A **77**, 032311 (2008).
[18] M. O. Scully and M. S. Zubairy, *Quantum Optics* (Cambridge University Press, Cambridge, UK, 1996).
[19] S. L. Zhang and P. van Loock, Phys. Rev. A **84**, 062309 (2011).
[20] Stefano Pirandola and Seth Lloyd, Phys. Rev. A **78**, 012331 (2008).
[21] T. Opatrný, G. Kurizki, and D. G. Welsch, Phys. Rev. A **61**, 032302 (2000).
[22] S. Olivares, M. G. A. Paris, and R. Bonifacio, Phys. Rev. A **67**, 032314 (2003).
[23] A. Kitagawa, M. Takeoka, M. Sasaki, and A. Chefles, Phys. Rev. A **73**, 042310 (2006).
[24] M. Sasaki and S. Suzuki, Phys. Rev. A **73**, 043807 (2006).
[25] A. P. Lund and T. C. Ralph, Phys. Rev. A **80**, 032309 (2009).
[26] ShengLi Zhang, JianHong Shi, ChenHui Jin, XuBo Zou, BaoSen Shi, and GuangCan Guo, J. Opt. Soc. Am. B **30**, 1922 (2013).
[27] H. Takahashi, J. S. Neergaard-Nielsen, M. Takeuchi, M. Takeoka, K. Hayasaka, A. Furusawa, and M. Sasaki, Nat. Photon. **4**, 178 (2010).
[28] R. García-Patrón, J. Fiurášek, N. J. Cerf, J. Wenger, R. Tualle-Brouri, and P. Grangier, Phys. Rev. Lett. **93**, 130409 (2004).
[29] Tim J. Bartley, Philip J. D. Crowley, Animesh Datta, Joshua Nunn, Lijian Zhang, and Ian A. Walmsley, Phys. Rev. A **87**, 022313 (2013).
[30] Hyunchul Nha and H. J. Carmichael, Phys. Rev. Lett. **93**, 020401 (2004).
[31] Yury Kurochkin, Adarsh S. Prasad, and A. I. Lvovsky, Phys. Rev. Lett. **112**, 070402 (2014).